CrossMark

ORIGINAL PAPER

Soy protein isolate/cellulose nanofiber complex gels as fat substitutes: rheological and textural properties and extent of cream imitation

Lu Sun · Wenshuai Chen · Yixing Liu · Jian Li ·
Haipeng Yu

Abstract The desire for good health has been a major impetus to drive the development of protein-polysaccharide complexes as fat substitutes. In the present study, complex gels were developed using two widely abundant renewable resources, soy protein isolate (SPI) and cellulose nanofiber (CNF). The aim was to assess the effects of incorporating CNF into SPI on the rheological and textural properties of the resultant mixture, and its potential application as an imitation of cream. Four mixtures with different SPI:CNF ratios (20:1, 15:1, 10:1, and 7:1 w/w) but at the constant total solid content 8 % were formulated. The SPI–CNF mixtures with a higher CNF proportion showed higher viscosity, storage modulus, and loss modulus, and an easier gelation characteristic. The most similar textural properties between the SPI–CNF (7:1) mixture and cream were observed. When 10, 20, or 30 % of this mixture was added into ice cream to replace an equivalent amount of cream, the targeted low fat, low calorie, anti-melting, and textural properties were achieved.

Graphical Abstract
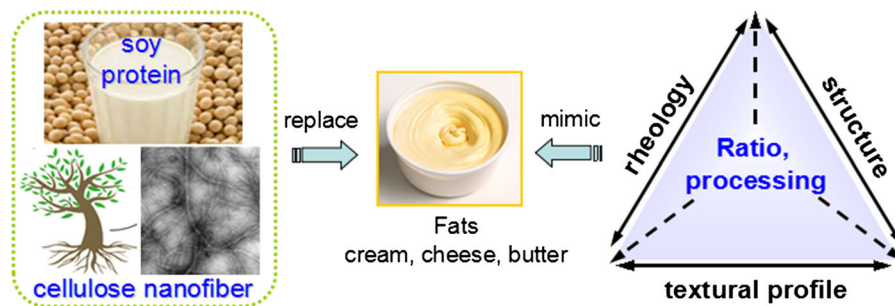
L. Sun · W. Chen · Y. Liu · J. Li · H. Yu (✉)
Key Laboratory of Bio-based Material Science and Technology of Ministry of Education, Northeast Forestry University, Harbin 150040, People's Republic of China
e-mail: yuhaipeng20000@aliyun.com

Introduction

Recently, consumers have highlighted their interest towards reduced or low- fat products because they

associated them with reduced risks of obesity and coronary heart diseases. The consumption of these products has become a way of life for many health-conscious people. Biopolymers derived from natural resources have attracted much attention, not only for their low cost and easy availability but also for their positive health effects, lower cholesterol, and reduced risk of dyslipidemia and cardiovascular diseases (Cengiz and Gokoglu 2005; Scholten et al. 2014). Plant proteins and polysaccharides are two important biopolymers, and they are also the main components influencing the flavor and texture of foods (Mehta et al. 2013).

Soy protein isolate (SPI) is a type of plant protein (≥90 % protein content), which has positive features such as solubility, swelling, gelling, and foaming, along with negative aspects such as low viscosity and limited mechanical strength (Nishinari et al. 2014). The processing forms of SPI are emulsions (Wagner and Gueguen 1999) and gels (Guerrero et al. 2011), and SPI can be combined with hydrophilic and hydrophobic materials to modulate their composition and properties (Song et al. 2011). Several studies have reported the use of SPI in edible films (Ou et al. 2005; Cho et al. 2010), packaging films (Guerrero et al. 2011), filtration membranes (Xu et al. 2012), adhesives (Xiao et al. 2013), tissue engineering, and drug delivery (Reddy and Yang 2011). In addition, SPI has been commonly used as a food supplement. Gelling and emulsifying were extremely common properties used in the development of food (Totosaus et al. 2002; Hua et al. 2003). The addition of polysaccharides considerably affects the emulsion stability of SPI through the rheological modification of the aqueous medium and interaction with the protein molecules (Li et al. 2007; Wang et al. 2011; Pan et al. 2015). The mixture of polysaccharides and SPI provides a taste similar to fat and with less energy. The mixture can be plied to various food products, particularly those meant to mimic and replace fat (Tolstoguzov 1991; Corredig et al. 2011). Nonetheless, removal of fat may cause negative effects on structure, texture, and flavor.

Cellulose, a semi-rigid polysaccharide that is generally known as dietary fiber, is commonly used in protein-polysaccharide complexes. Many physicochemical and physiological functions of cellulose and its derivatives have been reported, including water retention, rheological modification, emulsion stabilization, cholesterol level reduction, and bowel function improvement (Wu et al. 2009; Schmitt and Turgeon 2011). Hydroxypropyl methylcellulose (HPMC) was used to impart creaminess, lubricity, air entrapment, and moisture retention to baked goods and frozen desserts (Perez-Gago et al. 2005). Carboxymethyl cellulose (CMC) was used as a potential fat substitute in dairy and baked products as well as in low-fat meat products (Su et al. 2010). Microcrystalline cellulose (MCC) is another commercial cellulose derivative that has been successfully used as a fat substitute in hamburgers and sausages. It appears to have a good performance with respect to physiological functions while yielding low fat and low energy (Wang et al. 2013; Gibis et al. 2015).

Cellulose nanofiber (CNF) is a nanoscale cellulose derivative, which can be nanofibrillated from lignocelluloses using high-pressure homogenizers, grinders, blenders, or high-intensity ultrasonicators (Klemm et al. 2011; Dufresne 2013). The unique properties of CNF have been discussed in several studies and include low density, high aspect ratio, high strength, biocompatibility, and biodegradability (Moon et al. 2011; Chen et al. 2014). In addition to the abovementioned advantages, CNF also shows more valuable qualities as a rheological modifier and in self-assembly. It was found that the abundant hydroxyl groups and high aspect ratios favor the formation of hydrogen bonds and cause a critical gel concentration as low as 1.0 wt% (Chen et al. 2013). Therefore, CNF is a concerned material to replace the traditional cellulose derivatives and shape new-type biopolymer foods or composites (Moon et al. 2011; Abdul Khalil et al. 2012). The incorporation of CNF into SPI can lead to physicochemical alterations on the mixtures (Wang et al. 2006; Arboleda et al. 2013). Extrinsic factors that affect the formulation process include the pH, temperature, SPI to CNF ratio, total solid content, and ionic strength. The dynamic characteristics and textural properties of the formed SPI–CNF mixtures are also determined by the abovementioned factors (Song and Zhang 2008). Therefore, if some of these factors are ignored, the quality of many products will not meet the consumer's expectations.

In this study, we used the CNFs isolated from wood powder in combination with SPI, anticipating more apparent improvements in rheology and texture than those induced by the use of traditional cellulose derivatives. In order to control the gelation process and understand the relationship between the property and network structure of the formed SPI–CNF

mixtures, the changes of viscoelastic properties were monitored by the use of dynamic rheometry. The measurements were carried out at different mixing ratios and reaction temperatures. The texture of the resultant mixture was investigated, aiming to mimic and replace the fat cream. Finally, the ice creams having 10–30 % of cream fats replaced by an equivalent amount of SPI–CNF mixture were formulated and characterized.

Materials and methods

Materials

SPI from defatted soybean flour was purchased from Fonterra Co-operative Group Ltd (Auckland, New Zealand). The protein content in the SPI flour was 87.8 %. Poplar (*Populus ussuriensis*) wood powder sieved under 60-mesh was used as the raw cellulose source to fabricate CNF. The salt, hydrochloric acid, and sodium hydroxide were purchased from Tianjin Kermel Chemical Reagent Co., Ltd.

Preparation of CNF suspension

The preparation of CNF was mainly divided into purification step and fibrillation step (Chen et al. 2011). First, wood powder was subjected to a cyclic treatment with acidified sodium chlorite solution at 75 °C for 1 h to remove lignin. Subsequently, the sample was dissolved in 2 wt% potassium hydroxide at 90 °C for 2 h to leach hemicelluloses. To obtain purer cellulose fibers, the sample was further treated with 1 wt% sodium chlorite solution under acidic conditions (pH = 4–5) at 75 °C for 1 h and then treated with 5 wt% potassium hydroxide at 90 °C for 2 h. After purification, the resultant purified cellulose fibers (1 wt%) were ultrasonicated with an ultrasonic generator (JY99-IIDN, Ningbo Scientz Biotechnology Co., China) at 1200 W for 30 min, and resulted in 1.0 wt% CNF suspension. Before mixed with SPI solution, the 1.0 wt% CNF suspension was adjusted to 2 wt% by evaporation a portion of water.

Preparation of SPI–CNF mixtures

SPI flour was dissolved in distilled water, and the solution was magnetically stirred at room temperature for 3 h and stayed at 4 °C overnight to allow complete hydration. According to the SPI:CNF ratio of 20:1, 15:1, 10:1, and 7:1 (w/w) in Table 1, a certain amount of 14.0 wt% SPI solution was mixed with another amount of 2.0 wt% CNF suspension. The mixtures were then subjected to heating at 90 °C for 30 min, and obtained the SPI–CNF complex gels.

Formulation of reduced-fat ice creams

The ice cream was mainly formulated with whole milk (200 ml), light cream (125 ml), sugar (65 g), and egg. For each recipe, 10, 20 or 30 % cream in the ice cream was replaced by an equivalent amount of SPI–CNF (7:1) mixture. Their mixes were whipped and blended at 70 °C for 20 min, then pasteurized at 90 °C for 30 s, and finally cooled and immediately aged at 4 °C for 6 h. Batches of ice cream mix (20 L) were frozen in a continuous freezer (WCB ice-cream CS 100, Waukesha Cherry Burrell, Denmark; overrun: 100 %, outlet temperature: −5 °C). The ice creams were finally hardened at –40 °C and stored at −25 °C.

Rheological behavior test

The rheological measurement was performed on a rotational rheometer (AR2000, TA, USA). The sample was placed between the parallel plates with diameter 40 mm, and the slit distance was set to 1 mm. Filter paper was used to absorb the excess liquid, and silicon oil was used to seal the slit between the plates during the test. For frequency sweep, measurements were performed from 0.01 to 10 rad s^{-1} at 25 °C. For temperature sweeps, the strain was set to 1 %, and frequency was set to 1 Hz to ensure the linear viscosity range. Measurements were conducted from the initial temperature of 20 °C up to 90 °C at a heating rate of 5 °C min^{-1}, and then maintained at 90 °C for 30 min to ensure sufficient time for modulus to reach its equilibrium state. The samples were then cooled to 20 °C at a cooling rate of 25 °C min^{-1}. The storage modulus (G') and the loss modulus (G'') were recorded at different timepoints during the process. At a given oscillation frequency (ω), the dynamic complex viscosity ($\eta*$) could be obtained by combining the values of G' and G'' according to the following equation:

$$\eta* = \left[(G')^2 + (G'')^2 \right]^{1/2} / \omega$$

Table 1 The composition of the SPI–CNF mixtures

Sample	Total solid content wt%	SPI wt%	CNF wt%
SPI	8.00	8.00	–
$S_{20}N_1$-8	8.00	7.62	0.38
$S_{15}N_1$-8	8.00	7.50	0.50
$S_{10}N_1$-8	8.00	7.27	0.73
S_7N_1-8	8.00	7.00	1.00

Textural profile analysis (TPA)

Instrumental TPA (Model: TAXT2i, Stable Micro Systems, England) was used to measure the textural properties of the samples. For TPA, 30 ± 40 g sample was extended on a flat surface and carefully rolled to a thickness of about 10 mm. Each sample was compressed twice at 1 mm s^{-1} to 20 % of their original height, in a reciprocating motion to give a two-bite TPA curve, with an interval of 75 s between compressions. The following parameters were evaluated: hardness, adhesiveness, cohesiveness, springiness, gumminess, chewiness, and resilience.

Calorie calculation

Calorie is one of the important indices for evaluating the nutrition of food. According to the formulation of ice creams, the calories of every component were determined according to the Food Calorie Table, and calculated their total calories with reference to 100 g of ice cream.

Melting rate test

The ice cream samples were placed on a mesh grid (mesh size 1 × 1 cm) and allowed to stand at 30 °C, at constant humidity. The weight of the melting material passing through the screen was recorded as a function of time.

Observation of the microstructure

The SPI–CNF mixtures were freeze-dried into aerogel-type foams using a Scientz-10N freeze-dryer (Ningbo Scientz Biotechnology Co., Ltd., China). The cold trap temperature during the freeze-drying process was below −55 °C and the vacuum was below 15 Pa. Then the surface morphology was characterized by scanning electron microscopy (SEM, Sirion 200 microscope, FEI Inc., Eindhoven, Netherlands), operated at 20 kV in a high-vacuum mode. Before observation, the samples were coated with platinum.

Results and discussion

Influence of CNF content and heat treatment

The single disintegrated CNF prepared with a high-intensity ultrasonicator had a slender shape, with a width ranging in 2–20 nm (Fig. 1a) and a length exceeding 1 μm (Chen et al. 2015). Because a larger surface area and more hydroxyl groups were exposed, the CNFs are likely to crosslink and entangle together, which would facilitate the gel formation, particularly for the gel with a concentration above 1.0 wt% (Chen et al. 2013). When the CNF gel was mixed with the SPI solution, there was an improvement in apparent viscosity of the SPI–CNF mixtures (Fig. 1b). Heat treatment can result in the denaturation of SPI. Figure 1c demonstrates that after the heating, a further increase in viscosity and a decrease in the diffusion coefficient occurred in the SPI–CNF mixtures. Furthermore, an intertwined network formed (Fig. 1d) could hold certain components further the formation of the gelation state.

The rheological properties of the SPI–CNF mixtures can be determined with a rotational rheometer. The effects of oscillatory shear frequency on the viscoelastic properties of the SPI–CNF mixtures were evaluated and shown in Fig. 2. The control sample (pure SPI) had a weak gel state, corresponding to the behaviour of soft matter. The dynamic elastic modulus (G') and dynamic viscosity modulus (G'') of the mixtures with SPI:CNF ratios of 20:1 and 15:1 were similar to those of pure SPI and were frequency independent. Meanwhile, the G' and G'' values of the SPI–CNF (10:1 and 7:1) mixtures were much higher than those of pure SPI and those with a less CNF proportion and were frequency sensitive at the high-frequency band. These differences suggested that the addition of CNF could act as a rheological modifier and improve the viscoelasticity of the mixtures, even though the CNF amount was only one-tenth of SPI.
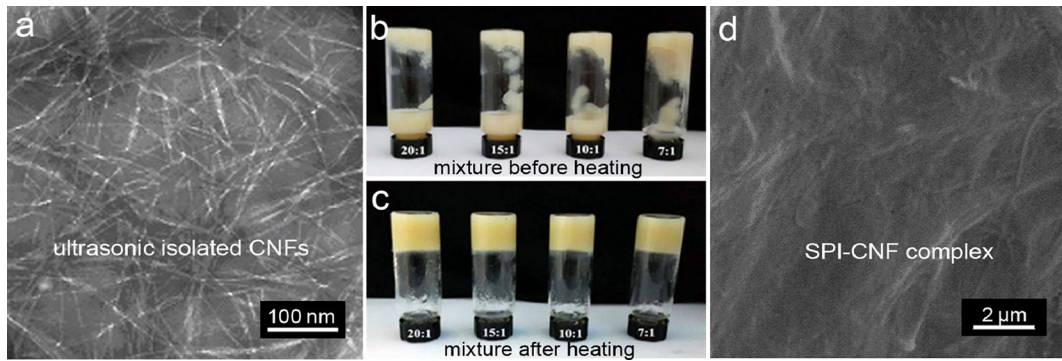
Fig. 1 a TEM image showing the ultrasonic disintegrated CNFs from wood powder; Pictures showing, **b** the low viscous state of the SPI–CNF mixtures before heating and **c** the gel state of the SPI–CNF mixtures after heating; **d** SEM image displaying the complex state SPI and CNFs
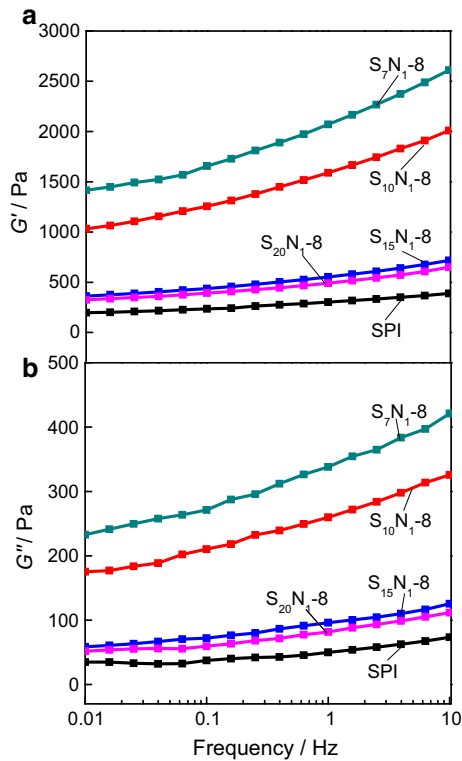

Fig. 2 a G' and **b** G'' curves of SPI and SPI–CNF mixtures as a function of oscillatory shear frequency
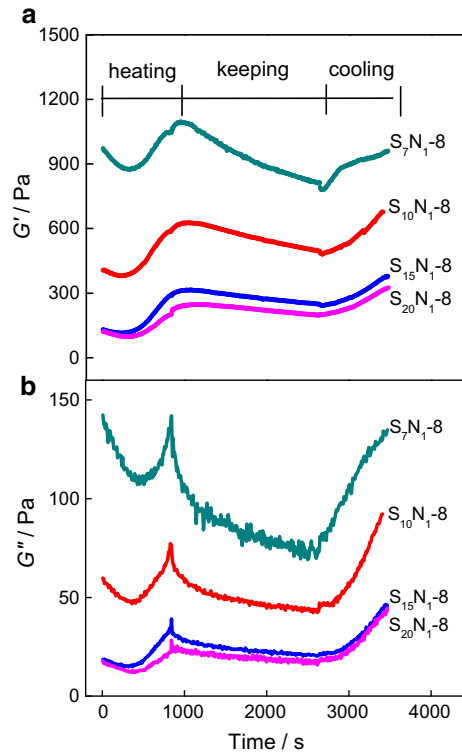

Fig. 3 Evolution of **a** G' and **b** G'' curves of the SPI–CNF mixtures at different temperatures and time periods

Similarly to other proteins, the primary condition for SPI gelation was a suitable concentration of protein with suitable heating conditions. The effect of temperature on the rheological properties of the SPI–CNF mixtures is shown in Fig. 3. In the whole process of temperature changing, G' and G'' appeared to be temperature-dependent, following the general behaviour observed in the SPI denaturation process. In the

initial SPI solutions, their surfaces were wrapped with a hydration film that was relatively stable. During the course of heating up, high temperature could intensify the thermal motion of SPI molecules and facilitate the structure transformation. The hydrophobic groups of the SPI molecules in the folded state were exposed, thus reducing the hydrophilic group outside the folded structure (Grinberg and Tolstoguzov 1997). The driving forces for gelation structure formation between the proteins and polysaccharides were the hydrophobic and electrostatic interactions of the components (Pan et al. 2015). Many reports have shown that cross-linking on a large scale appears after heating when the SPI concentration reached 8 % (w/v). The curve shapes of the mixtures with different SPI:CNF ratios were qualitatively similar but quantitatively different. The sample with a higher CNF proportion showed a higher variation in G' and G'' values with temperature. The rise of G' and G'' during the cooling process was perceived as a thermally reversible reaction (Nagano et al. 1994).

Comparison of TPA attributes

Some textural properties, including hardness, adhesiveness, chewiness, and resilience, often affect the final acceptance of targeted foods. To assess the textural properties of the resultant SPI–CNF mixtures, the instrumental TPA attributes of the SPI–CNF mixtures and cream were tested and compared (Fig. 4). According to the TPA values, almost no differences were found in springiness, cohesiveness, and resilience between the SPI–CNF mixtures and cream. Springiness and cohesiveness are the primary parameters of TPA analysis. Springiness is considered to be a measure of elasticity. After the first compression, the viscoelastic nature of the sample tended to return to its initial value. If the interval before the second compression was long enough to eliminate the stress, the shape recovery was close to 100 %. Cohesiveness, which characterizes the internal cohesion of the material, is only meaningful if the sample is partially deformed. Resilience, the rate of recovery after deformation, is correlated with most TPA parameters, except for adhesiveness. Low springiness, cohesiveness, and resilience stem from the viscous component nature of SPI. In the mixtures, CNF can have a similar effect as a stabilizer on the viscous liquid phase, thereby improving the texture. Figure 4
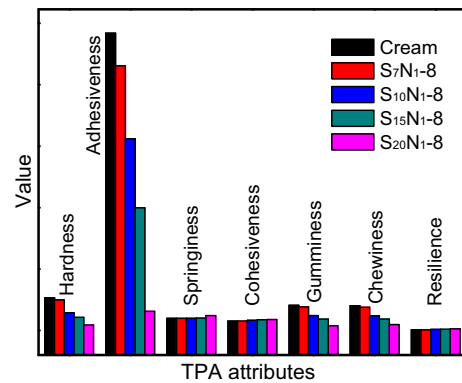

Fig. 4 Comparison of TPA attributes between the SPI–CNF mixtures and cream

also displays the small differences in hardness, gumminess, and chewiness. Among them, gumminess (hardness × cohesiveness) and chewiness (gumminess × springiness) are derived as secondary parameters. Furthermore, apparent differences appear in adhesiveness, which is generally evaluated as the maximum tensile force developed during adhesion, or as the cohesive rupture between two flat plates and the sample. Adhesiveness is always correlated with hardness. This is a consequence of the measuring test, in which adhesiveness is a property composed of surface adhesiveness, hardness, and cohesiveness. Thus, a decrease in adhesive force will be observed as hardness decreases. Through a comprehensive comparison of TPA attributes, we observed that the SPI–CNF (7:1) mixture showed the highest overall similarity to cream, which is also demonstrated by their textural profiles (see Figure S1 in supporting information).

Effects of adding the SPI–CNF mixture as a fat substitute in ice cream

The structure of ice cream has been identified as a three component foam made up of a network of fat globules and ice crystals dispersed in an aqueous phase having a high viscosity. In particular, fat appears to contribute largely to the properties of ice cream during whipping through the partially agglomerated continuous network of homogenized fat globules and freezing. For the reduced fat ice cream, low calorie, anti-melting, and acceptable texture are the most important properties. The challenge in working with

low-fat ice cream is related to the fact that if a high amount of fat is replaced, the fat globule network would be disrupted and this would affect the texture of the final product. Therefore, in this study, 10, 20, and 30 % cream in the ice cream were replaced by the SPI–CNF (7:1) mixture, respectively.

According to the formulation of ice cream, we queried out the calories of every component according to the Food Calorie Table and calculated its total calories in reference to 100 g of ice cream (Fig. 5). It can be seen that the calories decreased linearly with the increase in the percentage of cream replaced by the SPI–CNF mixture. This is because SPI provides only half the calories provided by fat, and almost no calories are provided by cellulose because it is hardly digested and absorbed by the human body.

The picture showing the melting process of the formulated ice creams is displayed in Fig. 6. The melting rate as a function of the percentage of cream replacement indicates that the melting rate depended on the ice cream formulation (Fig. 7). The presence of the SPI–CNF mixture caused an apparent decrease in the melting rate compared with that measured for the formulation without the replacer. The formulation with 10 % cream replacement presents the most remarkable impact. Water holding and structural stabilizer capabilities of the CNF–SPI mixture seemed to be the major contributors for the melting resistance of ice cream. In addition, the amphiphiles of the hydroxyl and amino groups can also help hold back both water and fat during the melting process. The microstructure of the SPI–CNF mixture after freeze-drying is exhibited in the Fig. 7 insert. Such homogeneous and honeycomb-like microstructures can

guarantee the structural stability and heat insulation for the ice crystals.

With respect to the textural aspect of the reduced fat ice creams, no obvious differences were observed in
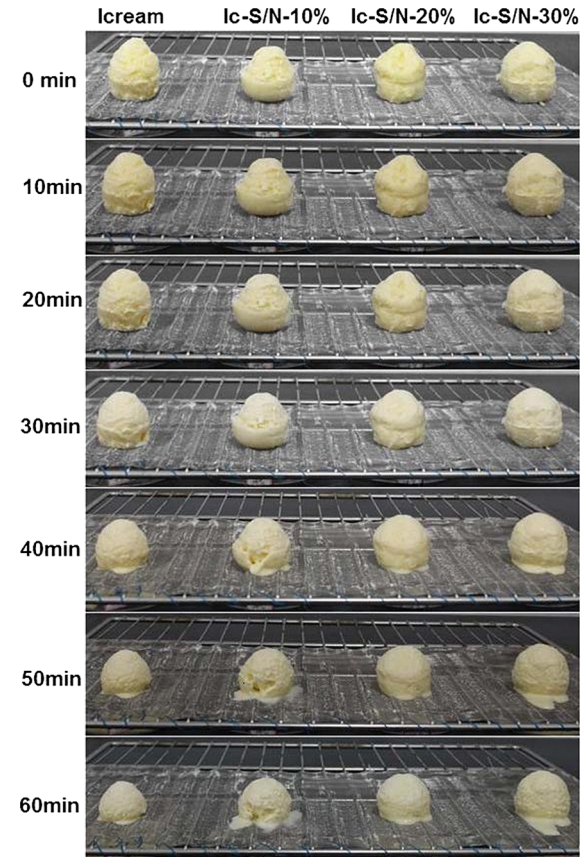
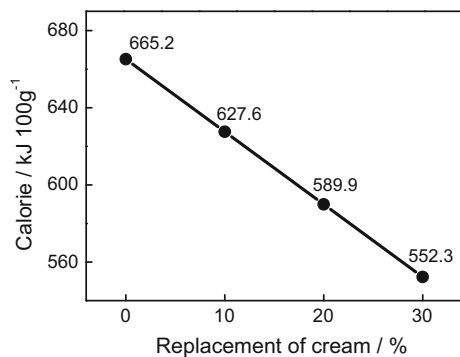**Fig. 6** The picture shows the melting process of the ice cream samples

Fig. 5 The calculated calories of the ice creams with the percentage of cream replacements
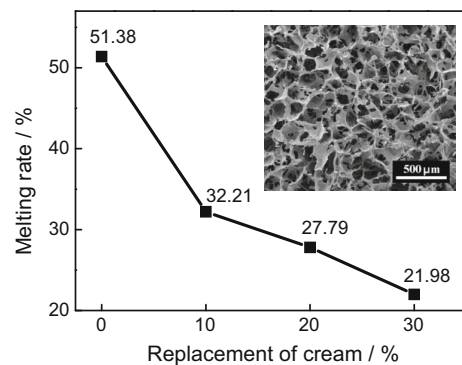
Fig. 7 Melting rate of the ice creams with the percentage of cream replacements
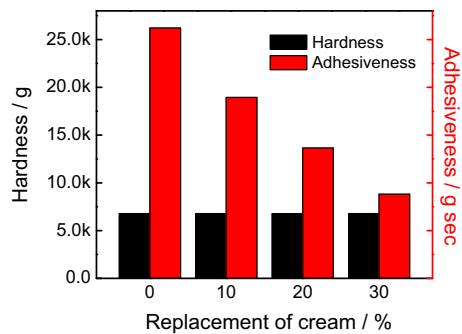
Fig. 8 Comparison of TPA attributes "Hardness" and "Adhesiveness" of the ice creams with the percentage of cream replaced by the SPI–CNF mixture

the TPA attributes, except for adhesiveness. For the sake of clarity, only hardness and adhesiveness were selected as representatives and are compared in Fig. 8. It can be seen that with the increase of the cream replacement, the adhesiveness value decreases, leading to a weakening of the soft and continuous feeling.

Conclusions

We ultrasonically disintegrated CNFs from wood powder and used them in combination with SPI as a structural stabilizer and rheological modifier. The resultant SPI–CNF mixtures had a higher viscosity and a larger modulus. The TPA attributes of the mixture with an SPI:CNF ratio of 7:1 were most similar to those of cream. The targeted effects of reduced fat, low calorie, anti-melting, and similar textural taste were achieved when this mixture was added to ice cream as a fat replacer, replacing 10 % of the cream.

References

Abdul Khalil HPS, Bhat AH, Ireana Yusra AF (2012) Green composites from sustainable cellulose nanofibrils: a review. Carbohydr Polym 87(2):963–979

Arboleda JC, Hughes M, Lucia LA, Laine J, Ekman K, Rojas OJ (2013) Soy protein–nanocellulose composite aerogels. Cellulose 20(5):2417–2426

Cengiz E, Gokoglu N (2005) Changes in energy and cholesterol contents of frankfurter-type sausages with fat reduction and fat replacer addition. Food Chem 91(3):443–447

Chen W, Yu H, Liu Y, Chen P, Zhang M, Hai Y (2011) Individualization of cellulose nanofibers from wood using high-intensity ultrasonication combined with chemical pretreatments. Carbohydr Polym 83(4):1804–1811

Chen P, Yu H, Liu Y, Chen W, Wang X, Ouyang M (2013) Concentration effects on the isolation and dynamic rheological behavior of cellulose nanofibers via ultrasonic processing. Cellulose 20(1):149–157

Chen W, Li Q, Wang Y, Yi X, Zeng J, Yu H, Liu Y, Li J (2014) Comparative study of aerogels obtained from differently prepared nanocellulose fibers. ChemSusChem 7(1):154–161

Chen W, Li Q, Cao J, Liu Y, Li J, Zhang J, Luo S, Yu H (2015) Revealing the structures of cellulose nanofiber bundles obtained by mechanical nanofibrillation via TEM observation. Carbohydr Polym 117:950–956

Cho SY, Lee SY, Rhee C (2010) Edible oxygen barrier bilayer film pouches from corn zein and soy protein isolate for olive oil packaging. LWT-Food Sci Technol 43(8):1234–1239

Corredig M, Sharafbafi N, Kristo E (2011) Polysaccharide-protein interactions in dairy matrices, control and design of structures. Food Hydrocoll 25(8):1833–1841

Dufresne A (2013) Nanocellulose: a new ageless bionanomatrial. Mater Today 6(16):220–227

Gibis M, Schuh V, Weiss J (2015) Effects of carboxymethyl cellulose (CMC) and microcrystalline cellulose (MCC) as fat replacers on the microstructure and sensory characteristics of fried beef patties. Food Hydrocoll 45:236–246

Grinberg VY, Tolstoguzov VB (1997) Thermodynamic incompatibility of proteins and polysaccharides in solutions. Food Hydrocoll 11(2):145–158

Guerrero P, Stefani PM, Ruseckaite RA, De la Caba K (2011) Functional properties of films based on soy protein isolate and gelatin processed by compression molding. J Food Eng 105(1):65–72

Hua Y, Cui SW, Wang Q (2003) Gelling property of soy protein–gum mixtures. Food Hydrocoll 17(6):889–894

Klemm D, Kramer F, Moritz S, Lindstrom T, Ankerfors M, Gray D, Dorris A (2011) Nanocelluloses: a new family of nature–based materials. Angew Chem Int Ed 50(24):5438–5466

Li JY, Yeh AI, Fan KL (2007) Gelation characteristics and morphology of corn starch/soy protein concentrate composites during heating. J Food Eng 78(4):1240–1247

Mehta N, Ahlawat SS, Sharma DP, Dabur RS (2013) Novel trends in development of dietary fiber rich meat products–a critical review. J Food Sci Technol 52(2):633–647

Moon RJ, Martini A, Nairn J, Simonsen J, Youngblood J (2011) Cellulose nanomaterials review: structure, properties and nanocomposites. Chem Soc Rev 40(7):3941–3994

Nagano T, Mori H, Nishinari K (1994) Effect of heating and cooling on the gelation kinetics of 7S globulin from soybeans. J Agr Food Chem 42(7):1415–1419

Nishinari K, Fang Y, Guo S, Phillips GO (2014) Soy proteins: a review on composition, aggregation and emulsification. Food Hydrocoll 39:301–318

Ou S, Wang Y, Tang S, Huang C, Jackson MG (2005) Role of ferulic acid in preparing edible films from soy protein isolate. J Food Eng 70(2):205–210

Pan H, Xu X, Tian Y, Jiao A, Jiang B, Chen J, Jin Z (2015) Impact of phase separation of soy protein isolate/sodium alginate co-blending mixtures on gelation dynamics and gels properties. Carbohydr Polym 125:169–179

Perez-Gago MB, Serra M, Alonso M, Mateos M, del Río MA (2005) Effect of whey protein- and hydroxypropyl methylcellulose-based edible composite coatings on color change of fresh-cut apples. Postharvest Biol Technol 36(1):77–85

Reddy N, Yang Y (2011) Potential of plant proteins for medical applications. Trend Biotechnol 29(10):490–498

Schmitt C, Turgeon SL (2011) Protein/polysaccharide complexes and coacervates in food systems. Adv Colloid Interfac 167(1–2):63–70

Scholten E, Moschakis T, Biliaderis CG (2014) Biopolymer composites for engineering food structures to control product functionality. Food Struct 1(1):39–54

Song F, Zhang LM (2008) Enzyme-catalyzed formation and structure characteristics of a protein-based hydrogel. J Phys Chem B 112(44):13749–13755

Song F, Tang DL, Wang XL, Wang YZ (2011) Biodegradable soy protein isolate-based materials: a review. Biomacromolecules 12(10):3369–3380

Su JF, Huang Z, Yuan XY, Wang XY, Li M (2010) Structure and properties of carboxymethyl cellulose/soy protein isolate blend edible films crosslinked by Maillard reactions. Carbohydr Polym 79(1):145–153

Tolstoguzov VB (1991) Functional properties of food proteins and role of protein-polysaccharide interaction. Food Hydrocoll 4(6):429–468

Totosaus A, Montejano JG, Salazar JA, Guerrero I (2002) A review of physical and chemical protein-gel induction. Int J Food Sci Technol 37(6):589–601

Wagner J, Gueguen J (1999) Surface functional properties of native, acid-treated, and reduced soy glycinin. 2. Emulsifying properties. J Agric Food Chem 47(6):2181–2187

Wang Y, Cao X, Zhang L (2006) Effects of cellulose whiskers on properties of soy protein thermoplastics. Macromol Biosci 6(7):524–531

Wang Y, Li D, Wang LJ, Adhikari B (2011) The effect of addition of flaxseed gum on the emulsion properties of soybean protein isolate (SPI). J Food Eng 104(1):56–62

Wang Z, Sun X, Lian Z, Wang X, Zhou J, Ma Z (2013) The effects of ultrasonic/microwave assisted treatment on the properties of soy protein isolate/microcrystalline wheat-bran cellulose film. J Food Eng 114(2):183–191

Wu RL, Wang XL, Wang YZ, Bian XC, Li F (2009) Cellulose/soy protein isolate blend films prepared via room-temperature ionic liquid. Ind Eng Chem Res 48(15):7132–7136

Xiao Z, Li Y, Wu X, Qi G, Li N, Zhang K, Wang D, Sun XS (2013) Utilization of sorghum lignin to improve adhesion strength of soy protein adhesives on wood veneer. Ind Crop Prod 50:501–509

Xu X, Jiang L, Zhou Z, Wu X, Wang Y (2012) Preparation and properties of electrospun soy protein isolate/polyethylene oxide nanofiber membranes. ACS Appl Mater Inter 4(8):4331–4337